This paper reports a study into the influence exerted by the thermal flows of space environment on the deformation of the shell of a space inflatable platform with a payload. The mathematical model of the effect of temperature fluctuations on the mass-inertial characteristics of the space inflatable platform of an ellipsoidal shape has been improved.

The following assumptions were introduced to the model. The temperature distribution on the illuminated part and the unlit part of the shell is uniform. The gradient of the temperature difference between the illuminated and unlit parts is the same for all points of the shell. To determine deformations, a moment-free theory was used. The model of the space inflatable platform is a «rubber bullet» that works only for stretching and compression. All deformations are elastic.

The advantages and limitations of the use of the developed mathematical model have been determined. Computer simulation of the orbital motion of a space inflatable platform with a payload in a sun-synchronous orbit was carried out. The material of the platform shell is Kapton. Estimates of temperature fluctuations in the illuminated and unlit part of the shell and the temperature of the gas inside it were obtained. The dependence of elastic deformations on temperature was determined, taking into account the Young's modulus of the material. The influence of changes in gas pressure on the movement of payload attachment points and the change in the inertia tensor have been determined. The obtained results showed that the inertia tensor varies within the order of 10^{-5} kgm^2. The maximum deviation of the fastening points of the payload from the initial position on the illuminated part of the shell was about 10^{-6} m.

Considering the stability of the structure to the effects of heat flows of the space environment, the possibility of using space inflatable platforms as a means for separating a grouping of satellites has been shown

Keywords: space inflatable platform, payload, heat flows of the space environment, dispenser inertia tensor, elastic shell deformations

UDC 629.7
DOI: 10.15587/1729-4061.2022.266161

DETERMINING THE DEGREE OF EFFECT OF HEAT FLOWS ON THE DEFORMATION OF THE SHELL OF A SPACE INFLATABLE PLATFORM WITH A PAYLOAD

Erik Lapkhanov
Corresponding author
PhD, Researcher*
E-mail: ericksaavedralim@gmail.com
Oleksandr Palii
PhD, Senior Researcher*
Aleksandr Golubek
Doctor of Technical Sciences, Associate Professor
Department of Automated Control Systems
Oles Honchar Dnipro National University
Gagarina ave., 72, Dnipro, Ukraine, 49010
*Department of Systems Analysis and Control Problems
Institute of Technical Mechanics of the National
Academy of Sciences of Ukraine
and State Space Agency of Ukraine
Leshko-Popelya str., 15, Dnipro, Ukraine, 49005

Received date 10.08.2022
Accepted date 14.10.2022
Published date 31.10.2022

How to Cite: *Lapkhanov, E., Palii, O., Golubek, A. (2022). Determining the degree of effect of heat flows on the deformation of the shell of a space inflatable platform with a payload. Eastern-European Journal of Enterprise Technologies, 5 (1 (119)), 6–16. doi: https://doi.org/10.15587/1729-4061.2022.266161*

1. Introduction

Space technologies cannot be imagined without the use of spacecraft orbital groupings (OG). There are two main types of spacecraft OG [1]:

1. «Order» – spacecraft OG constantly ordered relative to each other in space. Each in the grouping adheres to a given program position relative to the others.

2. «Swarm» – spacecraft OG of a time-varying order that is within certain program boundaries of the grouping.

Spacecraft OG have a variety of purposes and can perform various tasks. These tasks include:

– construction of a global satellite communication system;
– construction of global Internet;
– remote sensing of the Earth;
– satellite navigation systems;
– commercial private spacecraft OG of various non-military tasks (for example, satellites for the agriculture, scientific satellites, monitoring of natural resources, etc.).

Thus, spacecraft OG of the «order» type is often used for remote sensing tasks of the Earth. This is explained by the convenience of determining the frequency of coverage of terrestrial areas during the orderly movement of spacecraft in one orbit with maintaining a fixed distance relative to each other [1]. At the same time, large groups of the «swarm» type with satellites in different orbits:

– significantly increase the frequency of coverage;
– increase the reliability of the operation of spacecraft OG;

– make it possible to track changes in dynamics in any territory of the Earth, almost in real time [2].

To put spacecraft OG into orbit, a variety of adapters and dispensers are used. Thus, adapters serve as mechanisms for attaching the spacecraft to the upper stages of launch vehicles (LV). The dispenser, in turn, can be separated from LV, maneuver, and set each spacecraft certain necessary parameters of the orbit at the time of separation. As a rule, dispensers have in their composition all the necessary systems instruments and devices to enable autonomous controlled flight.

However, the launch of each kilogram of payload (PL) into near-Earth orbits comes at a price whose value can be USD tens of thousands [3, 4]. At the same time, dispensers and adapters for launching a large number of spacecraft into orbit can have a significant mass. On the other hand, these devices must be equipped with a special withdrawal system from orbit, to limit the period of orbital existence of 25 years [5] after the end of active functioning. To this end, the dispenser must have a withdrawal system, which, for example, makes it possible to increase the ballistic coefficient. Given this, minimizing the mass of an adapter or dispenser is an urgent task and requires scientific investigation.

2. Literature review and problem statement

One of the well-known designs of the dispenser is a specialized modular dispenser developed by Spaceflight Inc. (Seattle, USA) for the upper stage of the Falcon-9 LV [6, 7] whose general view is shown in Fig. 1 [6, 7]. The dispenser is designed for simultaneous launch of spacecraft OG into orbit.

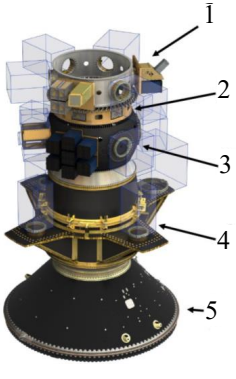

Fig. 1. Specialized modular dispenser for the upper stage of the «Falcon-9» launch vehicle: 1 — payload adapter based on the connecting ring developed by Boeing; 2 — module «CubeStack»; 3 — composite module «Hub»; 4 — Multi-cargo carrier; 5 — fitting for fastening on the upper stage of the Falcon-9 launch vehicle

The dispenser makes it possible to put into orbits of up to 64 spacecraft of the micro and nano class. The total mass of this dispenser, according to [7], reaches 1510 kg. However, despite the rather impressive size and mass of the dispenser, it does not have an active system of orientation and stabilization. This is explained by the possibility of minimizing inertia perturbations when the satellites are separated from the dispenser, which avoids a significant increase in angular velocities when moving around the center of mass and loss of stability. In turn, the use of a dispenser that does not have systems of orientation and stabilization will not make it possible to provide ultra-precise initial kinematic conditions for the separation of the spacecraft, which is necessary for the formation of OG of the «structure» type. Also, to limit the period of orbital existence, this dispenser must be equipped with a special aerodynamic device to increase the ballistic coefficient, which requires designing additional devices [7].

The next modification of Spaceflight Inc. dispensers is a Sherpa-FX5 type dispenser [8]. It makes it possible to bring about 190 kg of spacecraft to a sun-synchronous orbit close to a circular orbit with a height of 500 km. The natural weight of the dispenser (without satellite) – 125 kg. It does not have an engine system and an orientation and stabilization system. Given this, such a dispenser for the construction of spacecraft OG can be used only in conjunction with the upper stage of LV. Also, when using Sherpa-FX5, there are disadvantages similar to using the Falcon-9 LV dispenser (USA) [6, 7].

Of similar design is a dispenser of class SSMS PoC, developed by Arianespace (France) for the upper stage of «Vega» LV (European Union) [9] (Fig. 2). In the development and manufacture of SSMS class dispensers, the technology of honeycomb structures was applied. Thus, in [9] it is proposed to use six types of SSMS PoC dispensers for launching spacecraft of different classes into orbits.

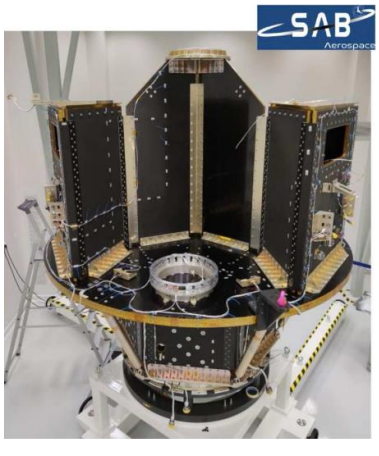

Fig. 2. Adapter for the upper stage of «Vega» LV [9]

Also, the SSMS PoC dispenser does not have an autonomous motion control system and is not separated from the upper stage of the Vega launch vehicle. On the one hand, this is an advantage since the upper stage and the dispenser make up the same system and can be removed from orbit using a single device. However, the upper stages of LV usually have significant masses, which may necessitate equipping such dispensers with powerful devices for removal.

Regarding Ukraine, DP «KB Yuzhnoye» named after M. K. Yangel (Dnipro, Ukraine) developed the LV upper stage «Cyclone-4» class for launching satellites into different orbits. This is a significant advantage, which allows for group launch of satellites into near-Earth orbits [10]. It uses the RD 861K engine unit (Ukraine), which has the ability to turn on 5 times when forming OG in different orbital ranges. Various adapters developed by DP «KB Yuzhnoye» are considered in [11]. All these adapters are also directly attached to the upper stage of the Cyclone-4 launch vehicle and are not separated after being put into orbit. Given this, such devices can be attributed only to the elements of fastening the spacecraft to the upper stage of LV, which do not have the possibility of autonomous operation.

In turn, WorldVu Satellites Limited (Cardiff, Great Britain) has developed a system for deploying space-

craft (Fig. 3, *a*) [12], which has many removable distribution modules. These modules are attached to each other, and each module carries a certain amount of spacecraft. Each module of the dispenser acts as a separate upper stage of the launch vehicle with its own power unit and deploys a subgroup of the spacecraft at the appropriate height and orbit. Since each dispenser module can deploy its own spacecraft away from other modules of the dispenser, the risk of collision between them is significantly reduced, which makes it possible to launch a large number of spacecraft in a safe, timely, and cost-effective way. This deployment system is described in [13] (Fig. 3, *b*).

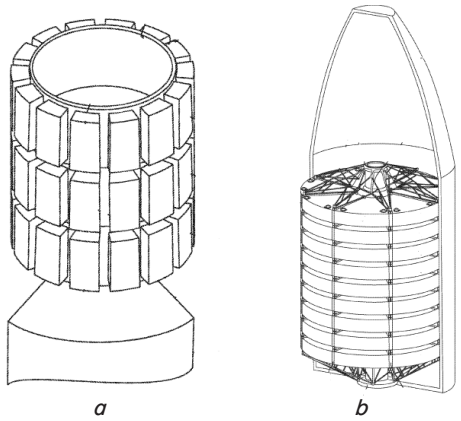

a *b*

Fig. 3. WorldVu Satellites Limited's satellite deployment system: *a* — deployment system with interchangeable distributed modules; *b* — deployment system of distributed dispenser system

Another company offering to manufacture the dispenser in the form of a fully autonomous module with its own set of service systems is the Raytheon Company (Waltham, Massachusetts, USA) [14]. This dispenser can also function independently after separating it from the upper stage of LV and continue to bring PL into the appropriate orbits.

The listed adapters and dispensers, as a rule, consist of composite materials, which in their composition have metallic elements that increase the mass of these systems. In turn, the approach to designing active dispensers that function as autonomous modules, like systems [12–14] based on space inflatable platforms (SIP) can reduce their mass characteristics. In addition, the use of this approach can reduce the cost and increase the ballistic coefficient of the dispenser. This, in turn, will make it possible not to equip the dispenser with an additional withdrawal system but to implement its removal only due to the action of the force of aerodynamic resistance of the atmosphere.

The level of scientific and practical consideration of the tasks to design and construct SIP is quite deep [15]. The most known applications of SIP are:

– inflatable space reflectors (Echo satellites) [15];

– inflatable antennas (SPARTAN experiment) [15];

– systems for storing and returning payload to Earth [15];

– inflatable modules for placing astronauts (BEAM) [16];

– inflatable rods for space systems distributed in space [17];

– systems for the removal of spent spacecraft from near-Earth orbits [18].

In addition, Nanoracks plans to launch the first inflatable autonomous space station by 2027, which allows up to four astronauts on board [19].

In turn, according to [15], the thickness of the shells of inflatable systems that do not involve astronauts on board is quite small (from one to several millimeters). Given this, mounting PL containers on an inflatable dispenser with this thickness is problematic. With this in mind, the authors of the work proposed a generalized concept of mounting PL on SIP using a frame of chain connections on top of inflatable modules [20]. However, the use of such a design can yield the mobility of the attachment points of PL under the influence of external factors of the space environment. One of these factors is temperature fluctuations when SIP moves through the illuminated and unlit part of the orbits, which can affect the gas pressure drops on the shell walls [21]. In turn, the mobility of PL attachment points on SIP will affect the change in the inertia tensor in flight and generate additional perturbations.

Thus, there is a task to assess the influence of the mobility of PL attachment points on the change in the mass-inertial characteristics of SIP.

3. The aim and objectives of the study

The purpose of this work is to determine the degree of influence of heat fluxes on the deformation of the shell of the space inflatable platform, the mobility of the payload attachment points, and the mass-inertial parameters of SIP with PL. This will make it possible to select the design parameters of SIP with PL at the initial design stage, taking into account the influence of heat fluxes on the change in the inertia tensor and the controllability of the system.

To accomplish the aim, the following tasks have been set:

– to improve the mathematical model of the influence of heat flows on the movement of the attachment points of PL and the equipment of the space inflatable platform arising from its deformation;

– to conduct computer simulation of the orbital motion of SIP with PL, taking into account the influence of heat fluxes on SIP;

– to investigate the influence of the movement of PL attachment points and equipment on the change of the inertia tensor of SIP.

4. The study materials and methods

The object of this study is methods for determining the effect of heat fluxes on space systems.

The main hypothesis of the study assumes the dependence of the mass-inertial characteristics (inertia tensor) of SIP with PL on the influence of thermal flows of the environment during the movement of SIP in the illuminated and unlit parts of the orbit.

Given that the set task of the study is nonlinear, complex, multidimensional, it is proposed to represent it in the form of a set of interconnected subtasks:

1. Determining the temperature of SIP shell and the gas inside it.

2. Determining the strength characteristics of SIP.

3. Determining SIP deformations.

4. Determining the current position of PL and equipment installed on the shell and the calculation of the mass-inertial characteristics of SIP.

5. Determining the current kinematic parameters of the translational orbital motion of SIP.

In the study of the effects of heat fluxes, the following assumptions were introduced:

a) the shape of SIP is ellipsoid;

b) the temperature of the parts of SIP that is under the sun's rays and in the shade is evenly distributed over the surface;

c) the gradient of the temperature difference between the illuminated and unlit parts is the same for all points of the shell;

d) when assessing the temperature effects on SIP, oriented movement in the Sun is considered; a change in the illumination of the surface, depending on the orientation, is not considered.

These assumptions can significantly simplify the rather complex calculations arising from the application of finite-element methods [22] in thermodynamics problems. In addition, when applying the assumption d), it is possible to conduct a study of the limiting case with the maximum heating of the shell of a certain part of SIP. For computer simulation of the orbital motion of SIP with PL, we apply software modules that we developed in the C/C++ programming language in the environment of Microsoft Visual Studio (Microsoft, USA) and Qt Creator for Linux (Trolltech, Norway).

5. Results of investigating the effect of heat fluxes on the deformation of the space inflatable platform with payload

5. 1. Mathematical model of the influence of heat fluxes deformation of the space inflatable platform

5. 1. 1. Coordinate systems

The following coordinate systems have been introduced:

a) orbital coordinate system (OCS) *OoXoYoZo*. Non-inertial right frame of reference with the *Oo* center in the center of SIP mass. The *OoZo* axis is directed to the center of the Earth, the *OoXo* axis lies in the plane of the orbit and is directed towards movement in the orbit (it forms an acute angle with the orbital velocity vector);

b) the coordinate system (BCS) bound to the center of SIP mass $O_BX_BY_BZ_B$. Its center O_B is located in the center of SIP mass, and the axes coincide with the main axes of inertia. The transition corresponds to the sequence of turns to the angles of roll, pitch, and yaw;

c) basic design polar coordinate system (BDPCS) $O_{BP}X_{BP}Y_{BP}Z_{BP}$ with the O_{BP} center in the geometric center of SIP. Coordinates are set by the design radius-vector of the current position, azimuth, and elevation angle;

d) basic design Cartesian coordinate system (BDCCS) $O_{BD}X_{BD}Y_{BD}Z_{BD}$. Its O_{BD} center is located in the geometric center of SIP. The axes coincide with the main axes of SIP;

e) a coordinate system that is connected to the movable payload mounting center (BMPL) $O_{BM}X_{BM}Y_{BM}Z_{BM}$. The O_{BM} center is at the point of attachment of the *i*-th payload. The axes are parallel in the direction of the axes of BCS.

5. 1. 2. Determining the temperature of the shell of the space inflatable platform from the outside and inside

The generalized structural scheme of SIP shell with PL fixed on it is considered as a three-layer wall (Fig. 4).

Taking into account the accepted assumptions, the following ratios were used to calculate the temperature of SIP [23]:

$$
\begin{aligned}
& m_{p.}C_{p.}\frac{dT_{p.}}{dt} = Q_{in.} - Q_{out.}, \\
& Q_{in.} = Q_{ext.p.} + Q_{int.p.}, \\
& Q_{out.} = \sigma\varepsilon_{p.}A_{sp.p.}T_{p.}^4, \\
& Q_{ext.p.} = E_s\alpha_{p.}A_{sol.p.} + E_a\alpha_{p.}A_{alb.p.} + E_p\varepsilon_{p.}A_{plan.p.},
\end{aligned}
\qquad (1)
$$

where $m_{p.}$ is the mass of the inflatable shell; $C_{p.}$ is the heat capacity of the upper layer of the inflatable shell; $T_{p.}$ is the surface temperature of the upper layer of the inflatable shell; $Q_{ext.p.}$ is the amount of heat transferred to the upper layer of the inflatable shell from the environment; $Q_{int.p.}$ is the amount of heat transmitted to the upper layer of the inflatable shell from the internal electrical equipment (taking into account external fasteners and heat screens of the payload, devices, and actuators, this value is proposed to be neglected); $\varepsilon_{p.}$ is the degree of blackness of the upper layer of the inflatable shell; $A_{sp.p.}$ is the area of the full surface of the upper layer of the inflatable shell; $\alpha_{p.}$ is the absorption coefficient (absorbency) of the upper layer of the inflatable shell; $A_{sol.p.}$, $A_{alb.p.}$, $A_{plan.p.}$ are the calculated areas of the upper layer of the inflatable shell that receive solar radiation, albedo radiation, and planetary radiation.

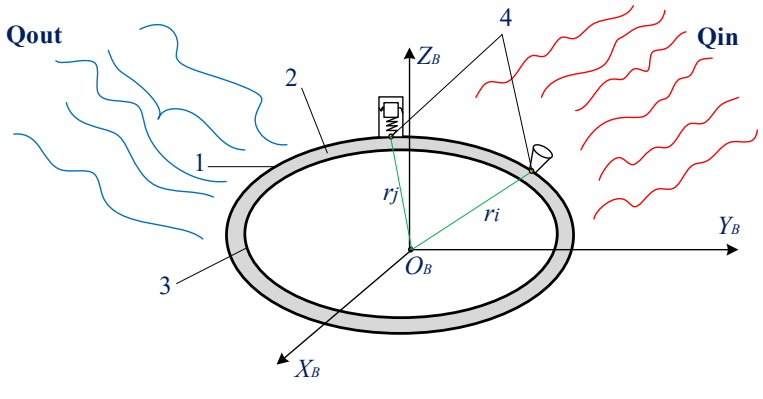

Fig. 4. Generalized structural diagram of a space inflatable platform with a payload, where *Qin* is the amount of heat entering the space inflatable platform from the environment; *Qout* — the amount of heat emitted by the space inflatable platform into the environment; *ri, rj* — positions of the *i*-th and *j*-th payload in the coordinate system connected to the center of mass of the platform; 1 — outer layer of the shell of the space inflatable platform; 2 — intermediate layer of the shell of the space inflatable platform (heat screen); 3 — inner layer of the shell of the space inflatable platform, 4 — attachment points of the *i*-th and *j*-th payload in the coordinate system connected to the center of mass of the platform

To determine the temperature of the illuminated and unlit part of SIP, equation (1) is represented as a system of the following two differential equations:

$$m_{p.il.}C_{p.}\frac{dT_{p.il.}}{dt}=E_s\alpha_{p.}A_{sol.p.il.}+E_a\alpha_{p.}A_{alb.p.il.}+$$
$$+E_p\varepsilon_{p.}A_{plan.p.il.}-\sigma\varepsilon_{p.}A_{sp.p.il.}T^4_{p.il.},\qquad(2)$$
$$m_{p.sh.}C_{p.}\frac{dT_{p.sh.}}{dt}=E_a\alpha_{p.}A_{alb.p.sh.}+$$
$$+E_p\varepsilon_{p.}A_{plan.p.sh.}-\sigma\varepsilon_{p.}A_{sp.p.sh.}T^4_{p.sh.},$$

where $T_{p.il.}$ is the temperature of the upper layer of the illuminated part of the shell; $T_{p.sh.}$ is the temperature of the upper layer of the shell in the shade; index «*il*» is the value of the parameters of the illuminated side of SIP; index «*sh*» is the value of the parameters of the shadow side of the inflatable platform.

It should also be noted that in the shadow part of the orbit, the values of E_s and E_a in equation (2) are zero. Taking into account the fact that the vacuum space between the layers of SIP is small and heat is transmitted due to thermal radiation, the procedure of calculating heat fluxes, which is given in work [23], is applied. Thus, heat fluxes from the upper layer of the wall of the illuminated and unlit part of SIP are determined by the equations:

$$E_{1.p.il.}=\varepsilon_{p.}\cdot c_0\cdot\left(\frac{T_{p.il.}}{100}\right)^4A_{p.il.},\qquad(3)$$
$$E_{1.p.sh.}=\varepsilon_{p.}\cdot c_0\cdot\left(\frac{T_{p.sh.}}{100}\right)^4A_{p.sh.},$$

where $E_{1.p.il.}$ is the heat flux from the illuminated wall; $E_{1.p.sh.}$ is the heat flux from the wall in the shade.

In turn, inside the material of the upper layer of the shell, heat is transferred due to thermal conductivity. Features of the gradient temperature difference between the shadow and solar sides of SIP are shown in Fig. 5.

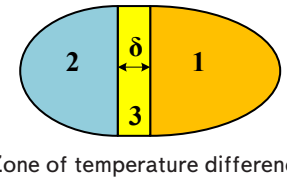

Fig. 5. Zone of temperature difference where: 1 – illuminated side of the shell; 2 – shadow side of the shell; 3 – temperature difference zone; Δ – width of the temperature difference zone

The heat transfer in the shell in the direction of the temperature difference gradient on the surface of the shell is considered. Taking into account the assumptions of uniform temperature distribution in zones 1 and 2 and the small thickness of the upper layer of the shell (Fig. 5), the equation of thermal conductivity in a flat wall under the boundary conditions of the second kind is used [23]:

$$q_{surf.}=-\lambda\mathrm{grad}\left(T_{surf.}\right),\qquad(4)$$
$$q_{surf.}=\frac{\lambda}{\delta}\left(T_{surf.il.}-T_{surf.sh.}\right),$$

where $T_{surf.}$ is the surface temperature of SIP shell; λ is the coefficient of thermal conductivity.

Accordingly, the outer layer transfers heat to the inner layer (the layers are not completely sealed, the interlayer space is a vacuum) of the shell wall, and, hence, changes its temperature. Taking this into account, the temperature of the inner layer of the shell of the illuminated and unlit part of SIP is calculated by using equations [23]:

$$E_{1.p.il.}=\varepsilon_{1-2}\cdot c_0\cdot A_{p.il.}\left[\left(\frac{T_{p.il.}}{100}\right)^4-\left(\frac{T_{p.il.in.}}{100}\right)^4\right],\qquad(5)$$
$$E_{1.p.sh.}=\varepsilon_{1-2}\cdot c_0\cdot A_{p.sh.}\left[\left(\frac{T_{p.sh.}}{100}\right)^4-\left(\frac{T_{p.sh.in.}}{100}\right)^4\right],$$

where $T_{p.il.in.}$ is the temperature of the inner wall of the illuminated part of the shell surface; $T_{p.sh.in.}$ is the temperature of the inner wall of the part of the surface of the shell located in the shade; ε_{1-2} – the reduced total value of the degree of blackness of the entire wall of SIP (Fig. 5).

Based on the fact that the thickness of the shell is several millimeters, the angular irradiation coefficients between the three layers of the shell will be considered equal to unity. Then, parameter ε_{1-2}, taking into account the interlayer screen, is calculated according to the equation:

$$\varepsilon_{1-2}=\frac{1}{\frac{1}{\varepsilon^0_{1-2}}+\left(\sum_{i=1}^{n}\left(\frac{2}{\varepsilon_{sc.i}}-1\right)\right)},\qquad(6)$$
$$\varepsilon^0_{1-2}=\frac{1}{\frac{1}{\varepsilon_{p.}}+\frac{1}{\varepsilon_{in.}}-1},$$

where ε^0_{1-2} is the reduced value of the degree of blackness between the outer and inner layer of the shell without taking into account the heat screen; $\varepsilon_{in.}$ is the degree of blackness of the inner layer of the shell; $\varepsilon_{sc.i}$ is the degree of blackness of the i-th screen of the intermediate layer of the shell.

Thus, the heat fluxes $E_{2.p.il.}$ and $E_{2.p.sh.}$ are determined, transmitted from the inner layer of the shell to the gas molecules inside. The temperature of the gas inside the shell is calculated using the equations given in [23]:

$$E_{2.p.il.}=c_0\cdot\varepsilon_{g.r}\left[\left(\frac{T_{p.il.in.}}{100}\right)^4-\left(\frac{T_{g.il.}}{100}\right)^4\right],\qquad(7)$$
$$E_{2.p.sh.}=c_0\cdot\varepsilon_{g.r}\left[\left(\frac{T_{p.sh.in.}}{100}\right)^4-\left(\frac{T_{g.sh.}}{100}\right)^4\right],$$

where $\varepsilon_{g.r.}$ is the reduced degree of blackness of the gas inside the shell; $T_{g.il.}$ is the gas temperature near the illuminated wall; $T_{g.sh.}$ is the temperature of the gas near the wall, which is in the shade. For further calculations of the effect of temperature changes on the change in the inertia tensor of SIP, the temperature of the gas inside the shell $T_{g.}$ is accepted as the average value near the illuminated wall (taking into account the zone of difference) and the wall in the shade:

$$T_{g.}=\kappa\left[\left(\frac{A_{p.il.}}{A_{p.}}+\frac{A_{p.diff.}}{A_{p.}}\right)T_{p.il.}+\left(\frac{A_{p.sh.}}{A_{p.}}\right)T_{p.sh.}\right],\qquad(8)$$

where $A_{p.il.}$ is the area of the illuminated surface of SIP; $A_{p.sh.}$ is the surface area in the shade; $A_{p.diff.}$ is the surface

area of the temperature difference zone; $A_{p.}$ is the full surface area of SIP; κ – dimensionless design parameter of heat transfer, calculated from formula:

$$\kappa = \frac{T_{g.il.} + T_{g.sh.}}{T_{p.il.} + T_{p.sh.}}.$$

Binding the temperature distribution to the surface of the shell is implemented using BDPCS and BDCCS. So, taking into account the assumption that SIP is always oriented to the Sun on one side, the following distinctions have been introduced between the unlit and illuminated zones of SIP shell, depending on the design azimuth in BDPCS:

1) from 90° to 270° – unlit area of SIP;

2) from 0° to 90° and from 270° to 360° – illuminated area of SIP;

3) the length of the difference zone is calculated in the flight of SIP in orbit, depending on the amount of heat received and emitted.

5. 1. 2. Determining the strength characteristics and deformations of the space inflatable platform

The following assumptions have been introduced:

1) the Young's modulus and the value of the boundary stresses when heating the shell of the satellite decreases by ℓ %;

2) the current values of the Young's modulus and the boundary stresses are calculated using tabulated dependences on the temperature of the material by interpolation.

Due to the fact that for systems such as SIP, the gas pressure inside the shell is two orders of magnitude higher than the pressure from the environment, a momentless theory is adopted to assess deformations. At the same time, SIP is considered a model of «rubber balloon», which has only elastic deformations depending on the internal pressure of the gas and works only for stretching and compression.

The deformations are considered at each i-th nodal point of fixing PL and equipment in BDCCS and are converted to BCS according to the formulas provided in [22]. Given this, in the vicinity of each nodal point, elementary areas and stress tensor are determined.

The deformation model is represented in the form of a system of equations:

$$\bar{\varepsilon}_i = D\mathbf{u}_i,$$

$$\mathbf{u}_i = \begin{bmatrix} \Delta x & \Delta y & \Delta z \end{bmatrix}^{\mathrm{T}},$$

$$D = \begin{bmatrix} \frac{\partial}{\partial x} & 0 & 0 & \frac{\partial}{\partial y} & 0 & \frac{\partial}{\partial z} \\ 0 & \frac{\partial}{\partial y} & 0 & \frac{\partial}{\partial x} & \frac{\partial}{\partial z} & 0 \\ 0 & 0 & \frac{\partial}{\partial z} & 0 & \frac{\partial}{\partial y} & \frac{\partial}{\partial x} \end{bmatrix}^{\mathrm{T}},$$

$$\bar{\varepsilon}_i = \begin{bmatrix} \bar{\varepsilon}_{i,x} & \bar{\varepsilon}_{i,y} & \bar{\varepsilon}_{i,z} & \gamma_{i,xy} & \gamma_{i,yz} & \gamma_{i,zx} \end{bmatrix}^{\mathrm{T}}, \qquad (9)$$

$$\begin{cases} \bar{\varepsilon}_{i,x} = \frac{1}{\mathrm{E}_i}\left[\sigma_{i,x} - \nu\left(\sigma_{i,y} + \sigma_{i,z}\right)\right], \\ \bar{\varepsilon}_{i,y} = \frac{1}{\mathrm{E}_i}\left[\sigma_{i,y} - \nu\left(\sigma_{i,x} + \sigma_{i,z}\right)\right], \\ \bar{\varepsilon}_{i,z} = \frac{1}{\mathrm{E}_i}\left[\sigma_{i,z} - \nu\left(\sigma_{i,y} + \sigma_{i,x}\right)\right], \end{cases} \begin{cases} \gamma_{i,xy} = \frac{\tau_{i,xy}}{G_i}, \\ \gamma_{i,yz} = \frac{\tau_{i,yz}}{G_i}, \\ \gamma_{i,zx} = \frac{\tau_{i,zx}}{G_i}, \end{cases}$$

where $\bar{\varepsilon}_{i,x}$, $\bar{\varepsilon}_{i,y}$, $\bar{\varepsilon}_{i,z}$ are the linear deformations at the i-th nodal point of SIP in BDCCS; $\gamma_{i,xy}$, $\gamma_{i,yz}$, $\gamma_{i,zx}$ are the shear deformations in the corresponding coordinate planes in the vicinity of the i-th nodal point of SIP in BDCCS; $\mathbf{u}_i$ is the vector of displacements of the deformed surface of the i-th nodal point of SIP in BDCCS; E_i is the modulus of longitudinal elasticity of the material at the i-th nodal point of SIP in BDCCS; G_i is the shear modulus at the i-th nodal point in BDCCS; ν – Poisson coefficient; $\sigma_{i,x}$, $\sigma_{i,y}$, $\sigma_{i,z}$ are the normal stresses acting on characteristic areas at the i-th nodal point of SIP in BDCCS; $\tau_{i,xy}$, $\tau_{i,yz}$, $\tau_{i,zx}$ – stresses directed along the tangent to the characteristic areas at the i-th nodal point of SIP in BDCCS.

In this work it is accepted that the gas presses on each elementary characteristic area of SIP shell in the same way while the pressure vector is directed along the normal to each elementary area. Given this, we have one linear deformation and one normal stress projection onto a characteristic area (Fig. 6). The values of other normal and tangential stresses are considered quite small, and their influence is proposed to be neglected.

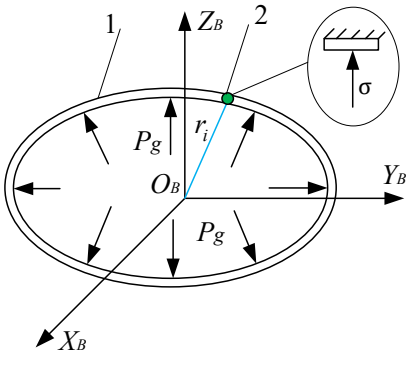

Fig. 6. Gas pressure on the inner walls of the shell of the space inflatable platform, where 1 is the shell of the space inflatable platform; 2 — payload mounting point; 3 — temperature difference zone; σ — stress on the characteristic area at the place of attachment of the payload, $P_{g.}$ is the gas pressure on the walls of the shell of the space inflatable platform

Thus, without the use of a boost system and thermoregulation, the gas pressure inside SIP shell is constant (isobaric mode [21]). However, in the isobaric process, the volume of gas is a function of its temperature $V_{g.}=f(T_{g.})$. Given the fluctuations in gas temperature during heating and cooling of SIP in the illuminated and unlit parts of the orbit, the volume of gas varies. With isobaric expansion of gas, the pressure on the walls of SIP shell increases.

Accordingly, with the application of the momentless theory [21] and the law of conservation of energy, elastic deformations of the shell arising during temperature fluctuations were found:

$$T_{g.} = \Delta W_{shell.}, \qquad (10)$$

where

$$T_{g.} = P_{g.} \frac{S_i}{S_{total.surf.}} \int_{V_1}^{V_2} \mathrm{d}V_{g.};$$

$$\Delta W_{shell.} = \frac{k\bar{\varepsilon}_i^{\,2}}{2} - \frac{k\bar{\varepsilon}_{i,0}^{2}}{2};$$

$$d\bar{\varepsilon}_i = \frac{\bar{\varepsilon}_i - \bar{\varepsilon}_{i,0}}{\Delta t};$$

$$k = \begin{cases} \dfrac{\ell \cdot \mathrm{E}_i \left(A_{p.il.} + A_{p.diff.}\right)}{l} & \text{– the illuminated part of the SIP shell,} \\ \dfrac{\mathrm{E}_i A_{p.sh.}}{l} & \text{– the SIP shell in the shade;} \end{cases}$$

$T_{g.}$ is the gas work during isobaric expansion; $P_{g.}$ – gas pressure; $V_{g.}$ – gas volume; V_1 – initial volume of gas; V_2 – current volume of gas; ΔW_{shell} is the change in the potential energy of the elastic shell of SIP; $\bar{\varepsilon}_i$ – elastic deformation of the shell at the point of attachment of the i-th PL in BCS; $\bar{\varepsilon}_{i,0}$ – initial elastic deformation of the shell at the point of attachment of the i-th PL in BCS; $d\bar{\varepsilon}_i$ – change in deformation at the point of attachment of the i-th PL in BCS; S_i – a characteristic area at the point of attachment of PL; $S_{total.surf.}$ is the area of the full surface of the inner wall of SIP shell; l is the thickness of SIP shell; Δt – change of time.

5. 1. 3. Determining the current position of the payload and equipment installed on the shell and the calculation of the mass-inertial characteristics of the space inflatable platform – 10–12 words

Features of determining the position of the payload on SIP, which has the form of a sphere, are set out in [23]. Given the use of an ellipsoidal SIP in the current study, the recalculation of payload positions is carried out in BDCCS.

The calculation of the mass-inertial characteristics of SIP is carried out according to the following algorithm:

1) calculate SIP deformations during temperature fluctuations during movement in the illuminated and unlit part of the orbit (2) to (11);

2) determine a change in the position of the mounting points of PL and the equipment in BMPL and recalculate the change in position in BDCCS;

3) recalculate the center of mass of SIP from PL to BDCCS according to the formulas given in [23];

4) calculate the transition from BDCCS to BCS and PL positions in BCS [23];

5) recalculate the inertia tensor using formulas from [23].

5. 1. 4. Determining the current kinematic parameters of the movement of the space inflatable platform

It has been suggested that the movement of SIP occurs under the influence of the following perturbations:

1) the gravitational potential of the Earth (5×5 harmonics are taken into account);

2) aerodynamic resistance of the Earth's atmosphere, the model NRLMSISE-00 is used [24];

3) solar pressure. The shadow model given in work [25] is used.

Due to the fact that the position of SIP in our paper is considered oriented by one side to the Sun at each point of the orbit, the features of angular motion are not considered.

In turn, the equation of orbital motion is written as follows [25]:

$$\left.\begin{aligned} \frac{dh}{dt} &= \frac{h^2}{\xi}\cdot T, \\ \frac{de_x}{dt} &= h\cdot\left[\begin{array}{l} S\cdot\sin F + T\cdot\left[(\xi+1)\cdot\cos F + e_x\right] - \\ -W\cdot e_y\dfrac{\eta}{\xi} \end{array}\right], \\ \frac{de_y}{dt} &= h\cdot\left[\begin{array}{l} -S\cdot\cos F + T\cdot\left[(\xi+1)\cdot\sin F + e_y\right] + \\ +W\cdot e_x\dfrac{\eta}{\xi} \end{array}\right], \\ \frac{di_x}{dt} &= \frac{h\cdot\tilde{\varphi}}{2\xi}W\cdot\cos F, \\ \frac{di_y}{dt} &= \frac{h\cdot\tilde{\varphi}}{2\xi}W\cdot\sin F, \\ \frac{dF}{dt} &= \frac{\xi^2}{h^3\mu} + W\cdot h\cdot\eta, \end{aligned}\right\} \quad (11)$$

where

$$e_x = e\cdot\cos(\omega+\Omega);\ e_y = e\cdot\sin(\omega+\Omega);$$

$$i_x = \mathrm{tg}(i/2)\cdot\cos\Omega;\ i_y = \mathrm{tg}(i/2)\cdot\sin\Omega;\ h = \sqrt{p/\mu};$$

$$\xi = 1 + e_x\cos F + e_y\sin F;\ \eta = i_x\sin F - i_y\cos F;$$

$$\tilde{\varphi} = 1 + i_x^2 + i_y^2;\ F = \omega + \Omega + \vartheta;$$

e is the eccentricity of the orbit; Ω – direct ascent of the ascending node; Ω – perigee argument; μ – gravitational constant, $\mu = 3{,}986\cdot10^5$ km^3/s^2; i – inclination of the orbit; ϑ – true anomaly; t – time; S, T, W – radial, transversal, and binormal perturbation accelerations.

The forces and accelerations generated by the action of perturbations are calculated according to the procedure described in [25]. Given this, the heat fluxes of solar radiation, terrestrial radiation, and albedo are determined based on the current position of SIP in orbit, which is calculated using model (11).

5. 2. Computer simulation of the orbital motion of a space inflatable platform, taking into account the influence of heat fluxes

Let SIP launch 9 spacecraft of remote sensing of the Earth into a sun-synchronous orbit: 3 CubeSat 16U class vehicles, 3 CubeSat 8U class vehicles, and three CubeSat 3U auxiliary devices. SIP also has 9 modules of its own technical equipment: sensors and controlling elements of the orientation and stabilization system. The orientation and stabilization system includes solar and stellar sensors, flywheel motors, and electromagnets. The SIP shell consists of a polyamide Kapton film with aluminum spraying and thermal screens with a thickness l=2 mm and an average density of 1400 kg/m^2, the Young's modulus for it is E=86.2 GPa [15].

Geometric parameters of the space inflatable platform:

– large semi-axis, oriented along the $O_{BD}X_{BD}$ axis in BDCCS: 3 m;

– the first small semi-axis oriented along the $O_{BD}Y_{BD}$ axis in BDCCS: 0.75 m;

– the second small semi-axis oriented along the $O_{BD}Z_{BD}$ axis in BDCCS: 0.75 m.

The parameters of the payload and technical equipment are given in Table 1.

The mass of the shell with flexible connections is 100 kg.

SIP has the following indicators of the degree of blackness of materials:

1) the degree of blackness of the upper layer of the shell $\varepsilon_{p.}$=0.01;

2) the degree of blackness of flexible solar panels $\varepsilon_{s.p.}=0.8$ (which occupies 20 % of the platform surface);

3) the degree of blackness of the inner layer of the shell $\varepsilon_{in.}=0.015$;

4) the degree of blackness of the interlayer heat screen $\varepsilon_{sc.i}=0.009$;

5) the degree of blackness of the gas (model value) $\varepsilon_g=0.03$;

6) $\ell=10\,\%$.

Table 1

Payload parameters

No. of entry	Title	Weight, kg	Design azimuth, degree	Design position angle, degree
1	CubeSat 16U+P-pod	20 (16+4)	0	0
2	CubeSat 8U+P-pod	10 (8+2)	45	0
3	CubeSat 3U+P-pod	5 (3+2)	90	0
4	CubeSat 8U+P-pod	10 (8+2)	135	0
5	CubeSat 16U+P-pod	20 (16+4)	180	0
6	CubeSat 8U+P-pod	10 (8+2)	225	0
7	CubeSat 3U+P-pod	5 (3+2)	270	0
8	CubeSat 3U+P-pod	5 (3+2)	315	0
9	CubeSat 16U+P-pod	20 (16+4)	0	45
10	Technical equipment	5	0	90
11	Technical equipment	8	0	–45
12	Technical equipment	5	0	–90
13	Technical equipment	7	180	45
14	Technical equipment	8	180	–45
15	Technical equipment	7	90	45
16	Technical equipment	8	90	–45
17	Technical equipment	7	270	45
18	Technical equipment	8	270	–45

The SIP shell has the following mechanical and gas characteristics:

1) Young's modulus $E=86.2$ GPa;

2) thickness $l=2$ mm;

3) the area of the full surface of the inner wall $S_{total.surf.}=22.68$ m^2;

4) gas pressure inside the shell $P_{g.}=0.01$ Pa;

5) the initial volume $V_1=7.0262$ m^3.

Taking into account the fact that SIP forms an orbital grouping of satellites for remote sensing of the Earth, a sun-synchronous orbit is considered [26] with the parameters given in Table 2.

It is assumed that after separation from the launch vehicle, SIP must separate all spacecraft within a day to form an orbital grouping. Taking this into account, a ballistic analysis of the translational movement of SIP at a given period of time (one day) was carried out. The nature of change in the elements of the orbit during flight over time is shown in Fig. 7–10.

Table 2

Orbit parameters of a space inflatable platform with a space load

Parameter	Value
Semi-major axis of the orbit, m	7,107,213
Eccentricity	0.001266
Orbit inclination, degree	98.432
Longitude of the ascending node, degree	278.043
Argument of perigee, degree	68.922
Latitude argument, degree	0.0

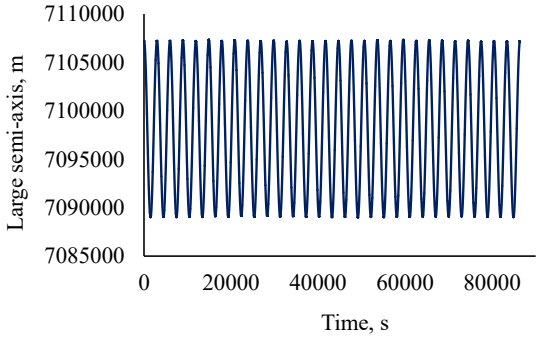

Fig. 7. The nature of change in the large semi-axis of the orbit

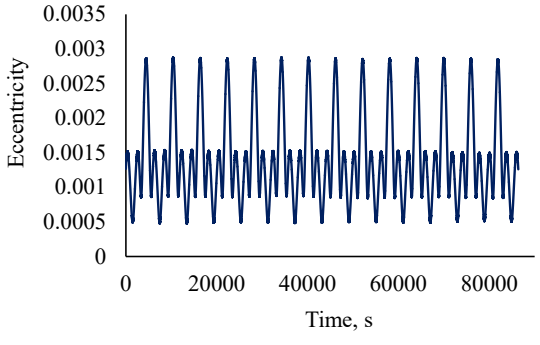

Fig. 8. The nature of change in the eccentricity of the orbit

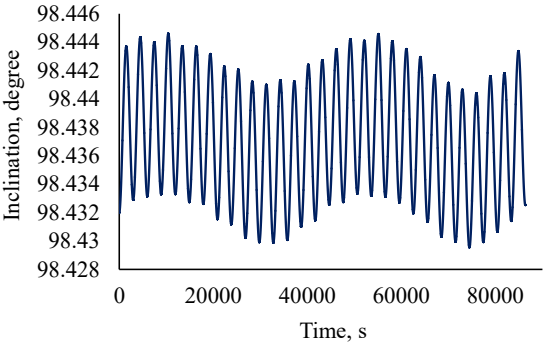

Fig. 9. The nature of change in the inclination of the orbit

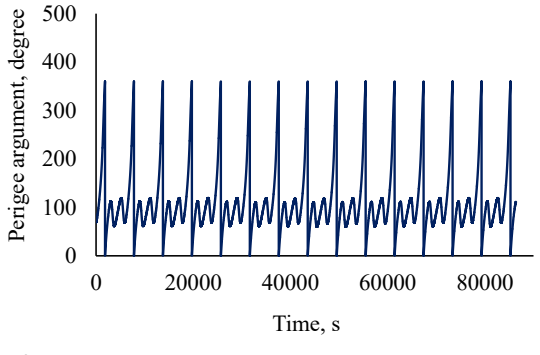

Fig. 10. The nature of change in the orbital perigee argument

To analyze the temperature effects, consider the movement of SIP with a focus on the sun. Thus, using formulas (1) to (11) and the procedure from [23], the influence of temperature factors is calculated. The change in temperature of the illuminated and shadow parts of SIP at the time interval of one day is shown in Fig. 11.

The above results (Fig. 11) demonstrate that the temperature of the illuminated part has a temperature difference

of about 100 K, which occurs when SIP moves along the shadow (minimum temperature) and illuminated part (maximum temperature) orbit (zone 1 in Fig. 5). At the same time, the temperature difference of a part of the platform that is always in the shade is about 35 K (zone 2 in Fig. 5). Taking this into account, the maximum temperature difference on the entire surface of SIP shell is 130–135 K. Calculation of the width of the temperature difference zone on SIP shell (zone 3 in Fig. 5) is shown in Fig. 12. In the zone of difference, temperature fluctuations at the border with the illuminated part corresponds to fluctuations in the temperatures of the illuminated part of the shell and with an increase in width Δ decreases to the amplitude of oscillation on the shadow side.

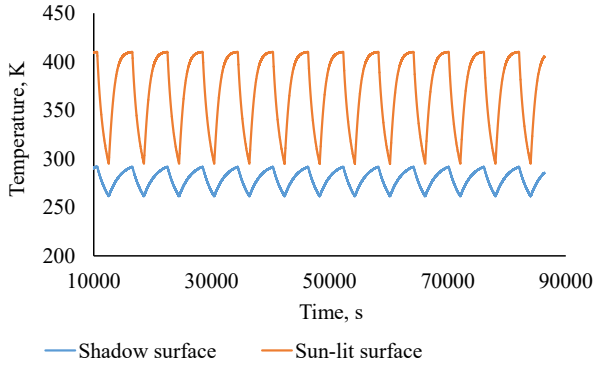

Fig. 11. The nature of temperature change in the illuminated and shadow part of the space inflatable platform of an ellipsoidal shape

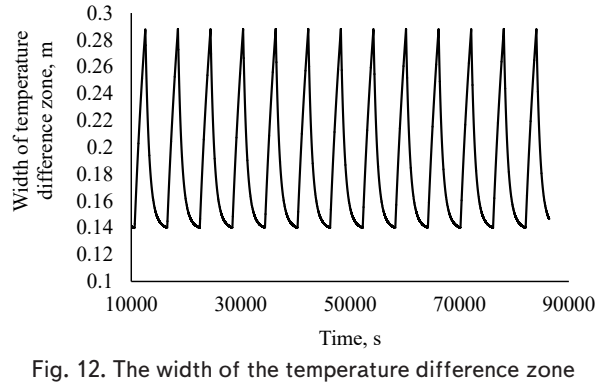

Fig. 12. The width of the temperature difference zone on the surface of the space inflatable platform

From the results shown in Fig. 12 it turns out that the width of the temperature difference zone also depends on the current position of SIP in the illuminated or unlit part of the orbit. Thus, with maximum heating of SIP shell (illuminated part of the orbit), zone 1 begins to transfer heat to zone 2, which is unlit. In this case, the temperature gradient is maximum, and hence the maximum temperature difference zone.

In turn, to reduce the pressure of the gas on the walls of the inflatable shell, it is necessary to reduce its temperature. Thus, with the use of thermal shielding properties of the shell, the temperature of the gas inside the shell reaches a maximum value of 300 K, which is 100 K less than the maximum temperature of the illuminated part of the inflatable platform (Fig. 13).

Thus, estimates of fluctuations in the surface temperature of SIP shell, fluctuations in gas temperature inside the shell were obtained, which makes it possible to analyze the deformations of SIP and the features of the change in the inertia tensor.

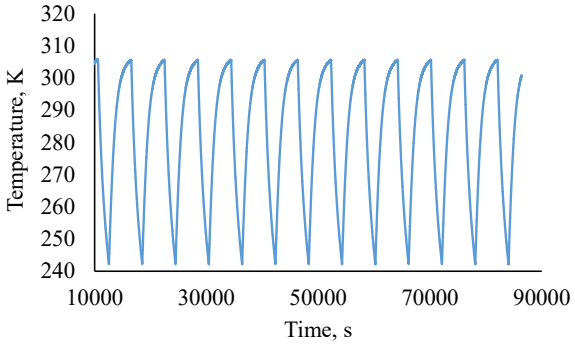

Fig. 13. The nature of change in the gas temperature inside the space inflatable platform

5. 3. Investigation of the effect of heat fluxes on the change in the inertia tensor of the space inflatable platform

With the use of models (9), (10) and calculation of the inertia tensor [21], the peculiarities of the influence of heat fluxes on the mechanical characteristics of SIP were determined. The change in the main axes of the inertia tensor under the influence of temperature factors in flight is shown in Fig. 14.

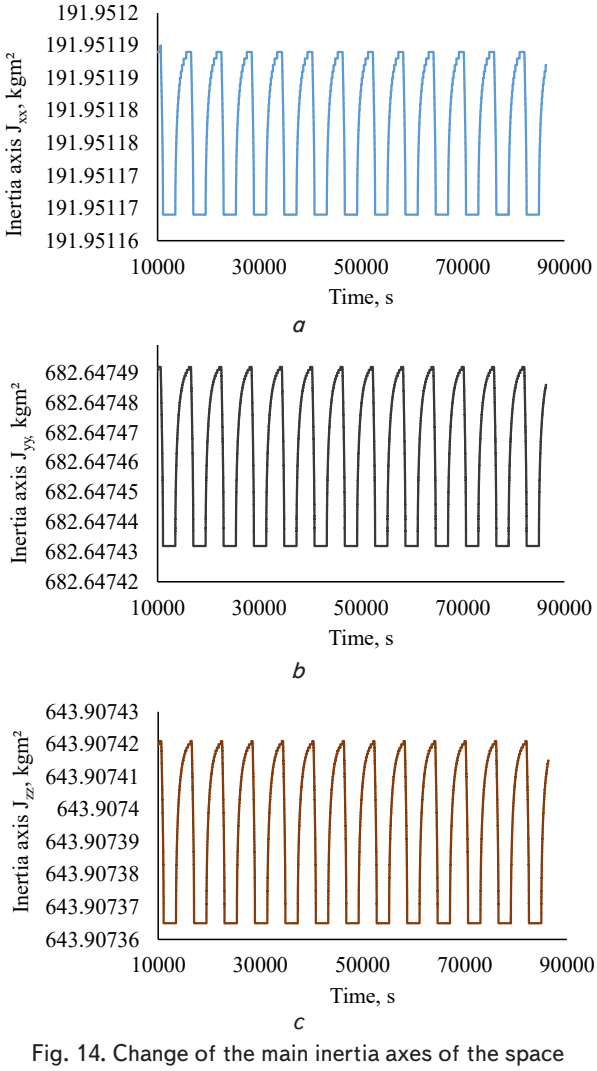

Fig. 14. Change of the main inertia axes of the space inflatable platform under the influence of temperature factors: *a* — change of the main axis of inertia *Jxx*; *b* — change of the main inertia axis *Jyy*; *c* — change of the main inertia axis *Jzz*

These results show that with given assumptions for modeling the deformations of SIP shell (application of the momentless theory), the amplitude of oscillations of the main axes of the inertia tensor is approximately 2×10^5 kg·m^2 (Fig. 14). Such fluctuations in the values of the main inertia axes are insignificant and coincide with the level of error in determining the inertia tensor at the design stage. Given this, such amplitudes of oscillations of payload attachment points will not create additional significant perturbations during the angular motion of SIP.

6. Discussion of results of applying the model of the influence of heat fluxes on the deformation of the space inflatable platform with payload

The mathematical model of calculating the mass-inertial characteristics and strength characteristics of SIP (1) to (11) has been built. In the mathematical model, certain assumptions have been introduced, which makes it possible to simplify it significantly. The advantage of this simplification is the convenience of integration into software products that allow solving the problems of designing modern SIPs. Due to this, the speed of design estimates of the influence of temperature fluctuations arising in the dynamics of the movement of SIP in orbit increases, to replace the inertia tensor and strength characteristics. In addition, the introduction of the assumption of heating certain defined areas of the surface of SIP without taking into account changes in the illumination of the surface, depending on the orientation, allows us to analyze the boundary case of heating the surface of SIP. This boundary case assumes the maximum effect of heat fluxes on this area during movement in the illuminated part of the orbit, and hence the maximum heating. Given this, the use of the model built makes it possible to quickly determine the design parameters of SIP shell in general form and can be applied to various types of its geometric shapes. In turn, this will allow for a quick analysis of the influence of heat fluxes on the mass-inertial characteristics of SIP with PL during movement in orbit. Thus, the dependence of change in the mass-inertial characteristics of SIP (inertia tensor, deformation) on the temperature during flight is necessary when designing a system of orientation and stabilization of controlled dispensers developed on the basis of SIP. Analysis of angular motion and selection of design parameters of the dispenser control system developed on the basis of SIP is the goal of further research.

However, the application of the mathematical model (1) to (11) has limitations. Thus, the use of model (1) to (11) does not make it possible to analyze the influence of heat fluxes for each element and node of SIP with PL. This requires the exact values of all thermal characteristics of materials, their exact geometric and mechanical properties, which, as a rule, are determined at the final stage of design during production. In this case, complex application packages are used that allow for analysis and simulation using finite-element methods [22], as well as special laboratory benches for verification of results;

The disadvantage of the study is the inability to integrate ballistics and navigation software into finished software products such as ANSYS (USA) where there are integrated tools that allow analysis using finite-element methods.

Thus, it is advisable to use the mathematical model (1) to (11) when choosing the design parameters of SIP with PL at the initial stage of design (conceptual design, pre-project research) where the possibility or impossibility of constructing a system is determined [27].

In further studies, when estimating heat fluxes for SIPs of different geometric shapes, the mathematical model can be sophisticated by introducing more nodal points to analyze temperature gradients. The degree of complexity of the model depends on the type of task and the design stage.

7. Conclusions

1. The mathematical model of the influence of heat flows on the movement of payload attachment points and the equipment of the space inflatable platform resulting from its deformation has been improved. The use of this mathematical model makes it possible to quickly determine the degree of influence of heat flows of the cosmic environment on the change in the mass-inertial characteristics (inertia tensor) of a space inflatable platform with a payload. It is advisable to apply the developed model at the stage of conceptual design, or pre-project research (Pre-Phase A (Conceptual study) according to NASA standards).

2. The built mathematical model of the influence of heat fluxes on the mass-inertial characteristics of SIP with PL was verified by computer simulation. With the use of ballistic-navigation libraries and a software model of the influence of heat fluxes on the deformations of SIP, computer simulation of the orbital motion of SIP with PL was carried out. The simulation made it possible to determine the peculiarities of the temperature difference of SIP shell, the gas inside SIP, and the change in the inertia tensor when moving along the solar and shadow sides of the orbit.

3. The influence of the movement of PL attachment points and equipment on the change of the inertia tensor of SIP was investigated. The results showed a rather small effect of temperature fluctuations on the inertia tensor of SIP (10^{-5} kg·m^2), which is explained by the sufficient strength characteristics of the selected material – Kapton. It is also determined that the deviations of PL attachment points from the initial position on the heated side of SIP shell are insignificant and amount to 10^{-6} m. Thus, given the stability of the structure to the effects of temperature flows of the space environment, the use of SIP as platforms for separating the grouping of satellites is possible.

Conflict of interest

The authors declare that they have no conflict of interest in relation to this research, whether financial, personal, authorship or otherwise, that could affect the research and its results presented in this paper.

Project funding

This work was carried out in accordance with agreement No. 04/01-2022(3) dated 04.01.2022 between the NAS of Ukraine and the Institute of Technical Mechanics of the National Academy of Sciences of Ukraine and the State Space Agency of Ukraine, which was concluded on the basis of the Order of the Presidium of the NAS of Ukraine dated 31.12.2021 No. 749. The research that led to the preparation of the manuscript was carried out at the expense of funding under the budget program «Support for the development of priority areas of scientific research» (CPCVK 6541230).

References

1. Pogudin, A. V., Gubin, S. V. (2017). Overview of the Characteristics and Methods of Creating a Grouping of Small Spacecraft. Otkrytye informatsionnye i komp'yuternye integrirovannye tekhnologii, 75, 57–67. Available at: http://nbuv.gov.ua/UJRN/vikt_2017_75_8
2. Parish, J. A. (2004). Optimizing coverage and revisit time in sparse military satellite constellations a comparison of traditional approaches and genetic algorithms. Monterey: Naval Postgraduate School, 125. Available at: https://ia800905.us.archive.org/12/items/optimizingcovera109451209/optimizingcovera109451209.pdf
3. Cobb, W. W. (2019). How SpaceX lowered costs and reduced barriers to space. The Conversation Media Group Ltd. Available at: https://theconversation.com/how-spacex-lowered-costs-and-reduced-barriers-to-space-112586
4. Wall, M. (2022). SpaceX raises launch and Starlink prices, citing inflation. Available at: https://www.space.com/spacex-raises-prices-launch-starlink-inflation
5. IADC Space debris mitigation guidelines. IADC-02-01. Revision 2. Available at: https://orbitaldebris.jsc.nasa.gov/library/iadc-space-debris-guidelines-revision-2.pdf
6. Schoneman, S., Roberts, J., Hadaller, A., Frego, T., Smithson, K., Lund, E. (2018). SSO-A: The First Large Commercial Dedicated Rideshare Mission. 32nd Annual AIAA/USU Conference on Small Satellites. Available at: https://digitalcommons.usu.edu/cgi/viewcontent.cgi?article=4073&context=smallsat
7. Taylor, B., Fellowes, S., Dyer, B., Viquerat, A., Aglietti, G. (2020). A modular drag-deorbiting sail for large satellites in low Earth orbit. AIAA Scitech 2020 Forum. doi: https://doi.org/10.2514/6.2020-2166
8. Sherpa-FX5 Orbital Debris Assessment Report (ODAR) (2021). Spaceflight, Inc. Available at: https://fcc.report/IBFS/SAT-STA-20210922-00127/13329215.pdf
9. Small Spacecraft Mission Service VEGA-C. User's Manual Issue 1 – Revision 0 (2020). Available at: https://www.arianespace.com/wp-content/uploads/2020/10/SSMS-Vega-C-UsersManual-Issue-1-Rev0-Sept2020.pdf
10. Degtyarev, A. V., Gorbulin, V. P. (2014). Evolyutsiya raketno-kosmicheskikh razrabotok KB «Yuzhnoe». Visn. NAN Ukrainy, 6, 51–76. Available at: http://dspace.nbuv.gov.ua/handle/123456789/69588
11. Makarenko, A. A., Mashchenko, A. N., Shevtsov, E. I. (2015). The development of modern means of spacecraft integration with a launch vehicle. Space Science and Technology, 21 (5), 18–23. doi: https://doi.org/10.15407/knit2015.05.018
12. Field, D. W., Askijian, A., Grossman, J., Smith, A. D. (2015). Pat. No. US 9463882. System and method for assembling and deploying satellites. No. 14/700504; declareted: 30.04.2015; published: 11.10.2016. Available at: https://scienceon.kisti.re.kr/srch/selectPORSrchPatent.do?cn=USP2016109463882
13. Field, D. W., Askijian, A., Grossman, J., Smith, A. D. (2015). Pat. No. US9718566B2. Stackable satellites and method of stacking same. No. 14/700,466. declareted: 30.04.2015; published: 01.08.2017. Available at: https://patents.google.com/patent/US9718566B2/en
14. Cosner, C. M., Baldwin, M. S. (2019). Pat. No. US11214388. Self-contained payload accommodation module. No. 16/243225; declareted: 09.01.2019; published: 04.01.2022.
15. Litteken, D. A. (2019). Inflatable technology: using flexible materials to make large structures. Electroactive Polymer Actuators and Devices (EAPAD) XXI. doi: https://doi.org/10.1117/12.2500091
16. Valle, G. D., Litteken, D., Jones, T. C. (2019). Review of Habitable Softgoods Inflatable Design, Analysis, Testing, and Potential Space Applications. AIAA Scitech 2019 Forum. doi: https://doi.org/10.2514/6.2019-1018
17. Wei, J., Yu, J., Tan, H., Wang, W., Eriksson, A. (2019). Design and testing of inflatable gravity-gradient booms in space. CEAS Space Journal, 12 (1), 33–41. doi: https://doi.org/10.1007/s12567-019-00256-w
18. Koryanov, V. V., Alifanov, O. M., Nedogarok, A. A., Uk, Y. S., Firsuk, S. O., Kulkov, V. M. (2021). Review of the technologies for development the inflatable brake device for deorbiting the space objects. AIP Conference Proceedings. doi: https://doi.org/10.1063/5.0036055
19. Martindell, C. (2022). Inflatable Space Station to Make Space Accessible. The American Society of Mechanical Engineers. Available at: https://www.asme.org/topics-resources/content/inflatable-space-station-to-make-space-accessible
20. Palii, O., Lapkhanov, E. (2021). Space inflatable platform to accommodate payload. InterConf, 323–328. doi: https://doi.org/10.51582/interconf.7-8.12.2021.037
21. Lapkhanov, E. O., Palii, O. S. (2021). Mathematical model for determining the design parameters of an inflatable payload-bearing space platform. Technical Mechanics, 4, 66–78. doi: https://doi.org/10.15407/itm2021.04.066
22. Karpilovskyi, V. S. (2022). Metod skinchennykh elementiv i zadachi teoriyi pruzhnosti. Kyiv: «Sofiia A», 275.
23. Beloglazov, V. P. (2016). Teoreticheskie osnovy teplotekhniki. Teploperedacha. Nizhnevartovsk: Izd-vo Nizhnevart. gos. un-ta, 118.
24. Picone, J. M., Hedin, A. E., Drob, D. P., Aikin, A. C. (2002). NRLMSISE-00 empirical model of the atmosphere: Statistical comparisons and scientific issues. Journal of Geophysical Research: Space Physics, 107 (A12), SIA 15-1-SIA 15-16. doi: https://doi.org/10.1029/2002ja009430
25. Fortescue, P., Swinerd, G., Stark, J. (Eds.) (2011). Spacecraft systems engineering. John Wiley & Sons. doi: https://doi.org/10.1002/9781119971009
26. Vinogradov, D. Yu., Davydov, E. A. (2017). Techniques of shaping steady near-circular solar-synchronous orbits for the long term existence of the spacecraft. Engineering Journal: Science and Innovation, 6 (66). doi: https://doi.org/10.18698/2308-6033-2017-6-1630
27. NASA Systems engineering handbook (2007). NASA SP-2016-6105 Rev2. Available at: https://www.nasa.gov/sites/default/files/atoms/files/nasa_systems_engineering_handbook_0.pdf